Preparation of indium tin oxide (ITO) thin film with (400) preferred orientation by sol–gel spin coating method

L. Dong[1] · G. S. Zhu[1] · H. R. Xu[1] · X. P. Jiang[1] · X. Y. Zhang[1] · Y. Y. Zhao[1] · D. L. Yan[1] · L. Yuan[2] · A. B. Yu[3]

Abstract

Tin doped indium oxide (ITO) thin films with (400) preferred orientation were fabricated by sol–gel spin coating method with metal indium and $SnCl_4 \cdot 5H_2O$ as indium and tin precursors, oxalic acid was used for synthesis of ITO sol as a stabilizer and methylcellulose as a binder. This study creatively combines thermal treatment at different temperatures with post-annealing treatment at 500 °C to prepare ITO thin films with enhanced conductivity and highly transmittance. It was found that the (400) preferred orientation growth strongly depends on thermal treatment temperature. Growth preferred orientation of the ITO thin films changed from (222) plane to (400) plane with the increase of thermal treatment temperature. The ITO thin film was thermal treated at 250 °C shows highly (400) preferred orientation, which exhibited an excellent conductivity (a low sheet resistance of 230 Ω Sq^{-1} and a low resistivity of 4.14×10^{-3} Ω cm) combining with a highly average transmittance of 85.12% and obtained the best figure of merit (8.68×10^{-4} Ω^{-1}).

1 Introduction

Indium tin oxide (ITO) film is a transparent conducting oxides (TCOs), which has a high electrical conductivity and high optical transparency in the visible spectrum. Therefore, it has been widely used as photoelectric devices [1, 2], thin–film sensors [3, 4], display panels and solar cells [5, 6]. There are many methods to fabricate ITO thin films such as magnetron sputtering [7], chemical vapor deposition technique [8], spray pyrolysis method [9], and sol–gel processing [10]. Generally, sol–gel method is the simplest, most cost-effective method, which can manipulate the doping levels conveniently.

Along with the higher performance requirements of electronic devices, ITO thin films are required to have better conductivity and higher visible light transmittance, especially for films prepared by sol–gel method. Many scholars

have done a lot of research on the preparation of ITO thin films by sol–gel method. Yang et al. [11] studied the Ag-ITO nanocomposite film to enhance the conductivity of transparent oxide film by sol–gel method. Xia et al. [12] investigated ITO films fabricated by spin coating methods on glass substrates with different ITO sources. Yadav et al. [13] reported the synthesis and characterization of nanocrystalline indium tin oxide (ITO) and its application as humidity and gas sensors.

Recently, it was found that the structure preference of the ITO films has a great influence on their optoelectronic properties. Shigwsato et al. [14] prepared the (400) preferred ITO films by DC magnetron sputtering and pointed out that the ITO films with (400) preferred orientation have better electrical properties. Kim et al. [15] prepared the (400) preferred ITO films by RF magnetron sputtering, also showed the ITO thin films with (400) preferred orientation demonstrate higher carrier concentrations and better mobility than the ITO thin films with (222) preferred orientation. To prepare preferred orientation ITO thin films, sputtering method has been widely reported and is easy to be obtained, however, there are few reports on sol–gel method. Liu et al. [16] used Sol–gel mothod prepared the ITO thin film, which has verified that the conductivity of films could be effectively improved by controlling the film's preferred growth orientation along (400) plane.

✉ G. S. Zhu
   zgs9539@163.com

1   Guangxi Key Laboratory of Information Materials, Guilin University of Electronic Science and Technology, Guilin 541004, China

2   School of Materials Science and Engineering, Xihua University, Chengdu 610039, China

3   ARC Hub for Computational Particle Technology, Monash University, Clayton, VIC 3800, Australia

There are many factors that affect the growth of ITO thin films fabricated by sol–gel method. Many scholars have systematically studied the effects of sol composition and annealing process on ITO thin films [10, 12]. However, the thermal treatment is easy to be neglected during the thin film preparation processing. In this work, we found that not only the stabilizer and binder, but also the thermal treatment temperature were crucial to the preferential growth of the films. To further improve the photoelectric properties of ITO thin films prepared by sol–gel method, we have proposed a method of combining thermal treatment under different temperatures with post-annealing treatment.

In this paper, we thermally treated the films for 20 min at 50 °C, 150 °C, 200 °C and 250 °C, respectively, and then processed by post-annealing in tubular furnace, to further increase the conductivity of the films, the thin films were annealed under Ar/5% H_2 continuously. Effect of thermally treated temperature on the structure, morphology and photoelectric properties of films were discussed in detail.

2 Experimental procedures

2.1 Preparation of ITO thin films

The ITO thin films were spin-coated on sodium calcium glass substrate, which was orderly ultrasonic cleaned by acetone, deionized water, absolute ethyl alcohol, and then dried with nitrogen. Metal indium and $SnCl_4 \cdot 5H_2O$ were used as indium and tin precursors. The sol preparation process is shown in Fig. 1. Firstly, 1.824 g metal indium was dissolved in 10 mL hydrochloric acid solution (5 mol L^{-1}), the solution was heated to 80 °C to dissolve metal indium. Heat the solution continuously until crystals are precipitated completely, then stop heating and dry the remains for use. Then 20 mL deionized water was added to the crystallized indium precursor and magnetic stirring for 2 h at 65 °C. Secondly, 0.62 g $SnCl_4 \cdot 5H_2O$ was added to the solution to meet the atom ratio of In:Sn to 9:1. Thirdly, oxalic acid was added as stabilizer and methyl cellulose as binder, the molar ratio of oxalic acid to indium ion is 1:10 and 0.4 g methyl cellulose was added to the solution. Finally, an appropriate amount of 0.4 mol/L of ammonia was added to adjust pH value approximately to 1–2, then some deionized water was added to make the concentration of the sol to about 0.4 mol/L. The transparent ITO sol was obtained by stirring at room temperature for 12 h and resting for 48 h.

The ITO sol with 0.4 M concentration was investigated through the following approach. At a spin-coating rate of 2000 rpm for 30 s, films with one layer could be obtained from the 0.4 M ITO sol. The films were thermally treated at 50 °C, 150 °C, 200 °C and 250 °C before a final annealing, and then annealing the ITO thin films in tubular furnace at
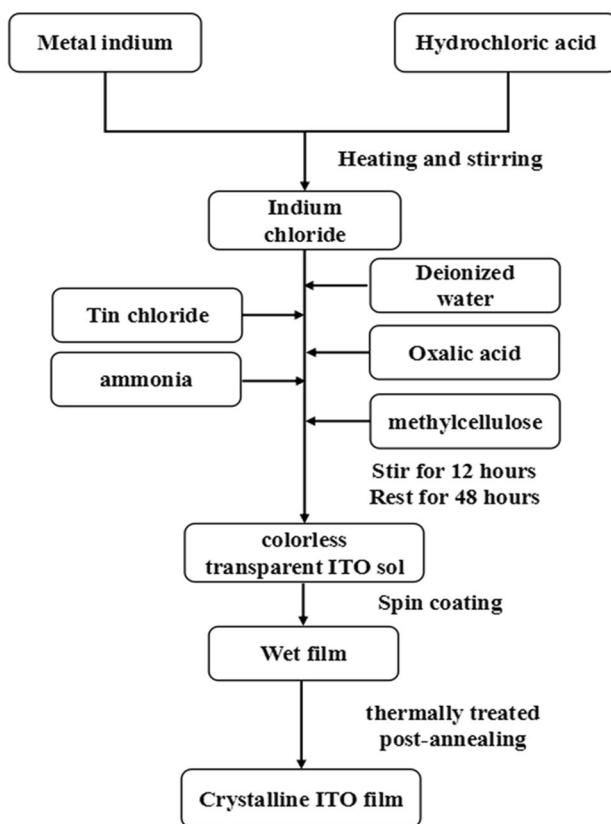

Fig. 1 The preparation process of ITO sol and ITO thin films

the temperature of 500 °C for 30 min with a heating rate of 5 °C min^{-1}, following annealing the ITO thin films in Ar/H_2 for 30 min to further decrease the resistivity. By studying the influence of the intermediate and final temperature on the structure, morphological and photoelectrical properties of the ITO thin films, the most promising sample in this study was presented.

2.2 Characterization techniques

TG/DTA investigation with a heating rate of 5 °C min^{-1} was carried out to study the mass loss and the phase transformation of the ITO sol. X-ray diffractometer (XRD-D8 Advance, Bruker Inc, Germany) with Cu Kα source (λ = 0.15405 nm) was used to characterize the crystalline structure, and the XRD data were collected in the 2θ range of 10°–80° by using the step scan mode with a step width of 0.01. The surface and cross-sectional morphologies of the ITO thin films were investigated using SEM (FE-SEM, FEI Tecnai-450, USA). The Electrical properties of ITO films were tested by four probe testing system and Hall effect test system. Transmission spectra was tested by ultraviolet–visible spectrophotometer (U-4100 type Hitachi, Japan). X ray photoelectron

spectroscopy was carried out to investigate the approximate content of oxygen element in the ITO films.

3 Results and discussion

3.1 Structure analysis

XRD patterns of the most promising samples were presented in Fig. 2a, all samples show strong peaks of the cubic In_2O_3 phase with the space group La3 and the results are in good agreement with the standard JCPDS data (PDF#06-0416), no separate peaks of SnO_2 or SnO were observed, which shows that tin ions have completely entered the lattice of indium oxide. XRD pattern shows two major diffraction peaks of (222) and (400). The main diffraction peak of ITO thin films changes from (222) to (400) with the increasing of thermally treated temperature. In particular, the film thermally treated at 250 °C shows the most intensity (400) diffraction peak. We believe that the reason for this phenomenon is that the oxalic acid decomposition preferentially consumes oxygen when the thermally treated temperature exceeds 150 °C. Therefore, the thin film is in a relatively oxygen-poor environment. During this thermally treated process, the thin films with (400) preferred seed crystals have been formed, then the seed crystal grows up during the annealing process. Kim [15] has studied the effects of oxygen partial pressure on the preferential orientation of ITO thin films, as the result shown, ITO thin film grown with pure Argon shows a preferential (400) plane orientation. Additionally, Kim [17] and Meng [18] have reported that the (400) plane possesses a lower surface energy than that of (222) plane, that means once a (400) preferred seed crystal formed, it would grow preferentially.

According to the DSC curves, we can observed a endothermic peak located at 100 °C, this is the decomposition of solvent in sol. Interestingly, the decomposition temperature of oxalic acid is between 150 and 160 °C, but we can't find any apparent endothermic peak from the DSC curve which shows on Fig. 2b. We believe that the decomposition of oxalic acid and crystallization of the film is very slow when they were thermally treated in the atmosphere at 200 °C or 250 °C, so the endothermic and exothermic process of the thin film is balanced. Besides, a slow and broad endothermic peak and exothermic peak are distributed at 300 °C and 500 °C respectively, which correspond to the decomposition of methylcellulose and the crystallization of the ITO films, respectively. It also can be seen from the TG curve that the sol has no mass loss beyond 500 °C.

The average crystalline sizes of ITO thin films were calculated from the full-width at half maximum of (222) and (400) diffraction peaks by using Scherrer's Equation [19].

$$d = \frac{K\lambda}{\beta \cos\theta}$$

where d is the main crystalline size, K is the shape factor taken as 0.943 (for non-spherical grains), λ is the wavelength of the incident beam, β is the full width at half maximum and θ is the Bragg's angle. The average crystalline size was calculated to be 31.17 nm, 46.85 nm, 53.86 nm, 61.76 nm for ITO thin films thermally treated at 50 °C, 150 °C, 200 °C, 250 °C. It has been reported that the (400) plane possesses a lower surface energy than that of (222) plane [17], as the results shown, the films with (400) preferred orientation grow larger.
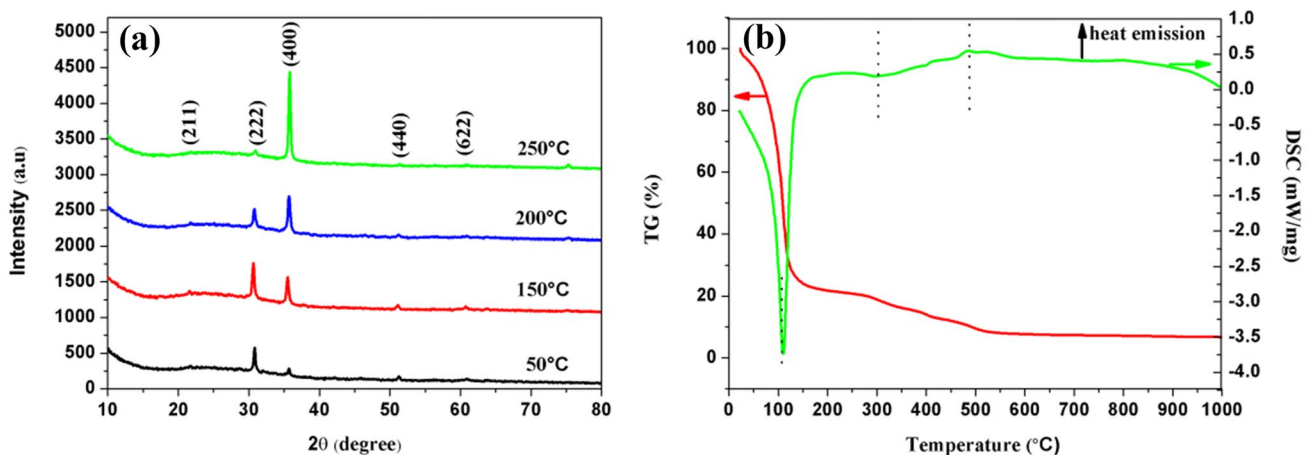

Fig. 2 **a** The XRD patterns of ITO thin films; **b** The TG/DSC curve of the ITO sol

3.2 Morphology analysis

The surface morphology, cross-section morphology and grain size of the ITO thin films were studied by scanning electron microscopy. Figure 3 shows the SEM images of the ITO thin films with different thermal treatment temperatures. Figure 3a shows the surface morphology of ITO thin film thermally treated at 50 °C, which exhibited macroporous surface. The film thermally treated at 50 °C only lost moisture and did not produce ITO seed crystalline grains, thus the crystallization and decomposition of methylcellulose were processing during annealing. To the best of our knowledge, the metal ions are surrounded by the long chain methylcellulose, though this is benefited to reduce the stress and strain of films [20], this also prevents densification between (222) preferential grains.

In comparison, the films thermally treated at higher temperatures have already produced a small amount of ITO seed crystalline. When thermally treated temperature exceeds 150 °C, the oxalic acid gradually decomposed. The decomposition of oxalic acid promotes the growth of ITO thin film with (400) preferential orientation. In general, (400) plane has a lower surface energy [17, 18], the grains of ITO thin film with (400) preferential gradually grow during annealing. Corresponding to Fig. 3d, it obviously shows different morphology compared with the other films, which
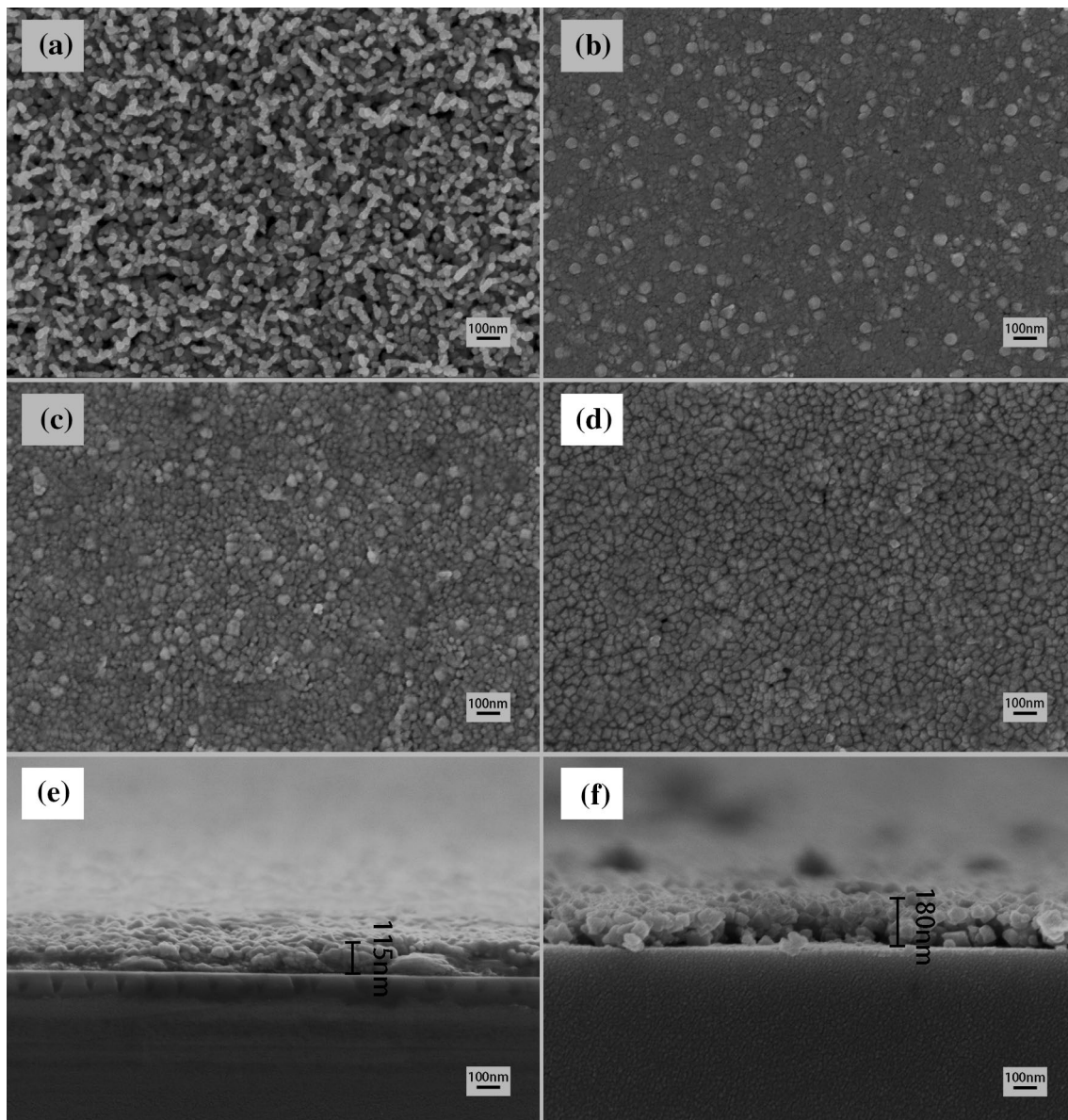

Fig. 3 SEM images of ITO thin films thermally treated at different temperatures **a** 50 °C; **b** 150 °C; **c** 200 °C; **d** 250 °C; **e** Cross-section of film thermally treated at 50 °C; **f** Cross-section of film thermally treated at 250 °C

presented as a close regularly arranged triangular-cone. We can observe from the surface morphology that the film with (400) preferred orientation has bigger crystalline grain.

Thus, we can observe from Fig. 3e, f that the thickness of film with (400) preferred orientation is thicker than film with (222) preferred orientation. The thickness of film thermally treated at 50 °C is about 115 nm, but the thickness is about 180 nm after thermally treating at 250 °C. In addition, the grain boundary decreases relatively, which reduces the trap points of grain boundary and further increases the conductivity of the film [21].

3.3 Optical performance analysis

The optical property was characterized by UV–Vis spectrophotometer. Figure 4a shows the transmission spectra of ITO thin films with different thermal treatment temperatures. Significantly, the ITO thin films are highly transparent in the visible region. All films have an average transmittance more than 85% in the visible region, which can meet the requirements of most photoelectric devices. We can see from Fig. 4a that the transmittance of film thermally treated at 50 °C has an advantage over that of film thermally treated at 250 °C. Considering that the surface of the film thermally treated at 50 °C has a large number of pores, which acts as a channel for visible light to pass directly through the film. Chuang Wang et al. [22] has found that the transmittance of wrinkled ITO thin film can be enhanced by the light-trapping at the valleys. Similarly, the transmittance of the thin film can be enhanced by the pores. Relatively, the film with (400) preferred orientation has a lower average transmittance, one reason for this phenomenon is due to free carrier absorption, resulting from the improved carrier concentration of film with (400) preferred orientation. Another reason

is server shrinkage of wet film at higher thermally treatment temperature, resulting in uneven surface of the film.

Figure 4b shows the energy band gap of films thermally treated at different temperatures. The energy band gap E_g can be calculated from the absorption coefficient, which can be calculated from the transmission spectra using equations [23]:

$$\alpha = \frac{1}{t} \ln \left(\frac{1}{T} \right)$$

where T is the transmission and t is the thickness of the films. The energy band gap of ITO film can be calculated from the following equation [23]:

$$ahv = A(hv - Eg)^m$$

where α is the absorption coefficient, h is the Planck's constant, ν is the frequency of incident light, A is constant, Eg is the energy band gap of material and m equals to 1/2 for direct semiconductors. The optical band gaps of films thermally treated at 50 °C, 150 °C, 200 °C, 250 °C are 3.48, 3.75, 3.65, 3.63 eV, respectively. We believe that increasing the number of carriers leads to increase in the Fermi level above the bottom of the conduction band, thereby causing an enlargement in the optical band gap of the ITO films. As the result shown, the film thermally treated at 150 °C presented a biggest energy band gap, which is benefited from its excellent carrier concentration.

3.4 Electrical performance analysis

The electrical performance of the films was analyzed by four-probe testing technique and Hall measurement system. Hall effect test datas are summarized in Table 1. Figure 5a exhibits the sheet resistance and figure of merit (FOM) of ITO thin films with different thermally treated temperature.
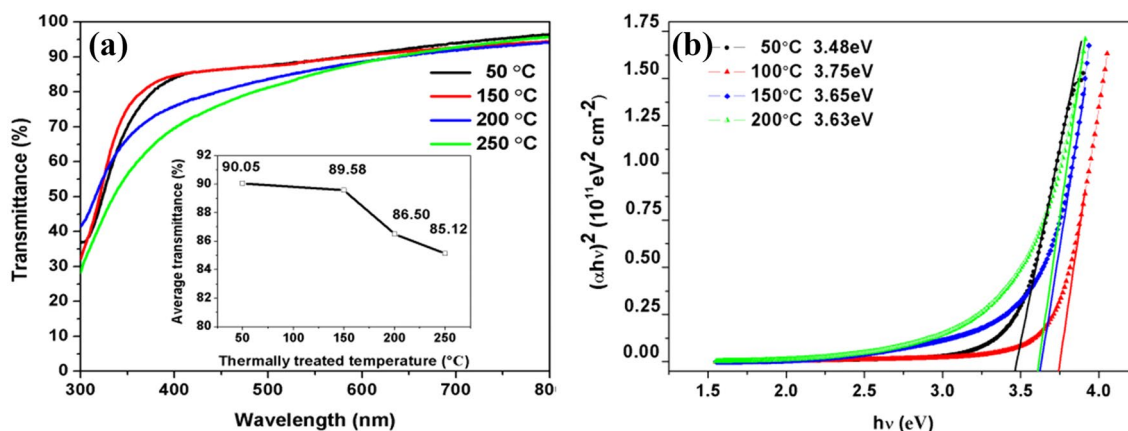

Fig. 4 **a** The transmittance of ITO thin films thermally treated at different temperatures; **b** The energy band gap of ITO thin films thermally treated at different temperatures

Table 1 Resistivity, carrier concentration and mobility of ITO thin films thermally treated at different temperatures

Thermally treated temperature (°C)	Resistivity (10^{-3} Ω cm)	Carrier concentration (10^{19} cm^{-3})	Mobility (cm^2 V^{-1} s^{-1})
50	8.39	9.80	7.59
150	6.30	13.0	7.63
200	4.48	11.0	12.68
250	4.14	10.2	14.80

It was found that the sheet resistance strongly depends on the structure of the thin films. The thin film with (400) preferential orientation has lower sheet resistance than film with (222) preferential orientation. Specifically, the sheet resistance of ITO film thermally treated at 250 °C is as low as 230 Ω Sq^{-1}. Recently, LIU Jiaxiang et al. [16] have prepared ITO film with (400) and (422) main diffraction peaks by sol–gel method, the 200 nm thick film has a relatively low sheet resistance (< 550 Ω Sq^{-1}). Hyun Cho et al. [24] has prepared ITO thin films by sol–gel method, the film that

was fired and annealed at 500 °C had a sheet resistance of 361 Ω Sq^{-1}. Compared with the results above, the electrical properties of the ITO thin films have been greatly improved. Figure 5b shows the resistivity, carrier concentration and mobility of ITO thin films, we believe that the improved conductivity of ITO thin films is related to the increasing of carrier concentration and mobility. As the results shown, the resistivity is decreasing from 8.39 to 4.14×10^{-3} Ω cm with the increase of thermal treatment temperature, which mainly due to the mobility increase from 7.59 to 14.8 cm^2 V^{-1} s^{-1}.

Figure 5c, d displays the fitting XPS narrow spectrum of O 1s for the ITO thin films which thermally treated at 50 °C and 250 °C. The results contain three components, located at 529.8 (529.9), 531.2 (531.5), and 532.3 (532.8) eV, respectively. The first peak is assigned to bulk oxide, the second peak corresponds to surface oxygen-deficient oxide, the last peak comes from the surface hydroxyl groups [25]. We can calculate from the O1s spectrum that the intensity ratio of oxygen-deficient of the films thermally treated at 50 °C and 250 °C is 0.54. From the results of XPS analysis, it can be seen that the oxygen hole content increases when the film
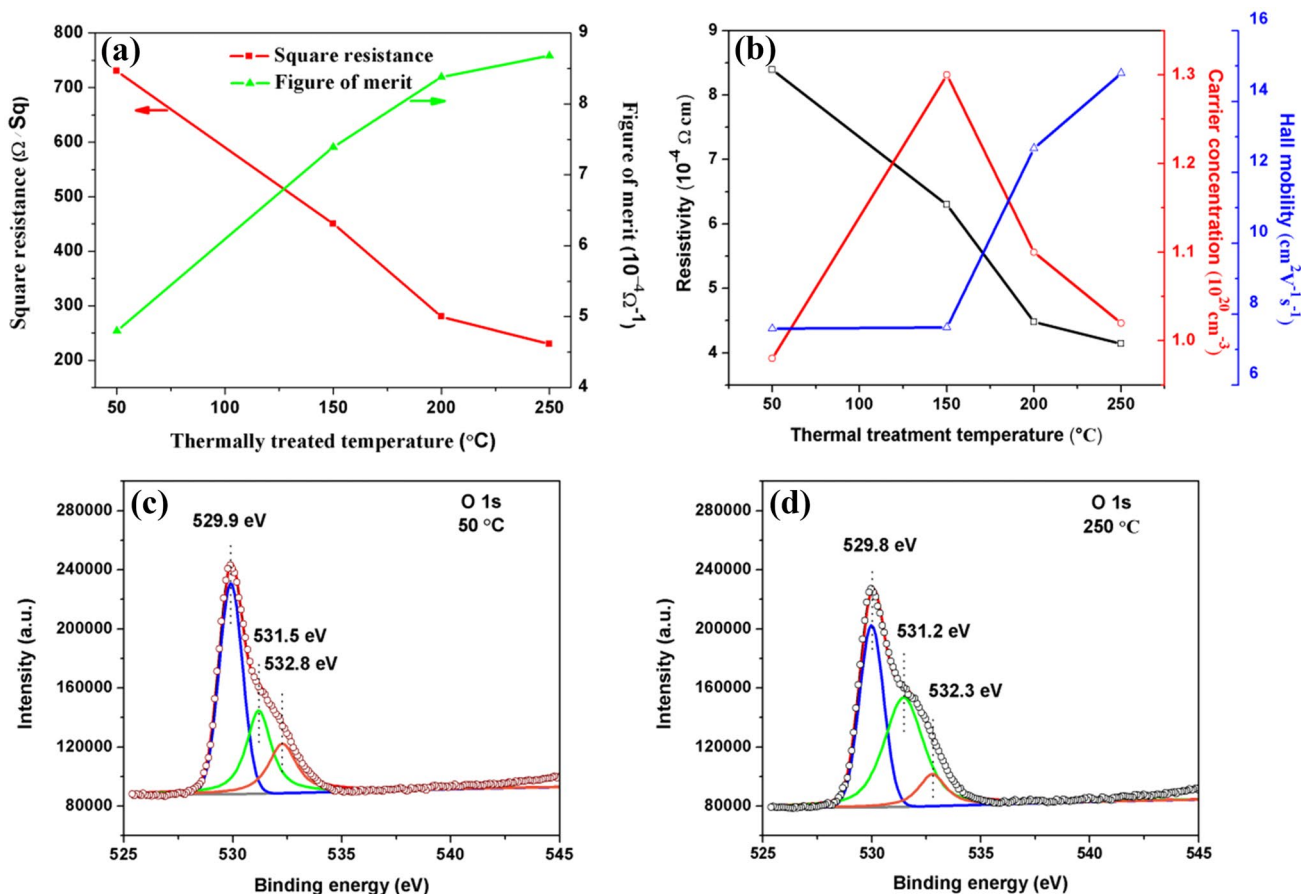

Fig. 5 **a** The sheet resistance and figure of merit (FOM) of ITO thin films at different temperatures; **b** Resistivity, carrier concentration and mobility of ITO thin films; **c**, **d** The XPS narrow spectrum of O1s for ITO thin films thermally treated at 50 °C and 250 °C

Table 2 Crystalline preferred orientation, sheet resistance, transmittance, and Hackee figure of merit of ITO thin films thermally treated at different temperatures

Thermally treated temperature (°C)	Preferred orientation	Sheet resistance(Ω Sq^{-1})	Average transmittance (%)	Figure of merit $\emptyset_H$ (10^{-4} Ω^{-1})
50	(222)	730	90.05	4.80
150	(222)	450	89.58	7.39
200	(400)	280	86.50	8.38
250	(400)	230	85.12	8.68

was thermally treated at 250 °C, which leads to an improvement in carrier concentration of the film.

The mobility of ITO thin films depends on several major factors [26, 27], including ionized impurity, lattice vibration and grain boundary scattering. In this study, grain boundary scattering is the main influence factor in the mobility of ITO thin films. Lee et al. [26] have reported that the increased grain size caused the increasing of electron mean free path, which is related to the decrease in the grain boundary scattering in the ITO films, in this case, grain boundary scattering is the main factor that limits Hall mobility. ITO thin film thermally treated at 250 °C with high (400) preferred orientation has larger grain size, which decreases the grain boundary scattering. As a result, this thin film exhibited a lowest sheet resistance (230 Ω Sq^{-1}) and a lowest resistivity (4.14×10^{-3} Ω cm). The relationship between the preferred orientation, square resistance, transmittance and figure of merit and annealing temperature of the films is shown in Table 2.

There is a competitive alternative between the transmittance and resistivity to produce TCO films by sol–gel process [26]. We use figure of merit (FOM) defined by [28]

$$\phi_H = \frac{T^{10}}{R_s}$$

To quantitatively evaluate the performance of ITO films thermally treated at different temperatures. Where T and R$_S$ each separately represent the transmittance and sheet resistance. The film thermally treated at 250 °C displays the best combination of conductivity and transparency, showing the highest figure of merit (8.68×10^{-4} Ω^{-1}).

4 Conclusion

ITO thin films with (400) preferred orientation were synthesized on sodium calcium glass substrate by sol–gel spin-coating method. The effect of thermal treatment temperature on the structure, morphology and photoelectric properties of ITO thin films have studied. The preferred orientation of the ITO thin films changed from (222) to (400) with the increase of thermal treatment temperature. The thin film thermally treated at 250 °C with (400) preferred orientation

has an average transmittance of 85.12%, a relatively low sheet resistance of 230 Ω Sq^{-1} and a low resistivity of 4.14×10^{-3} Ω cm. This sample shows the best figure of merit (8.68×10^{-4} Ω^{-1}). In this study, we controlled the preferential growth of thin films, thus the electrical properties of the films are improved effectively.

References

1. H.M. Lee, S.S. Kim, H.K. Kim, Artificially MoO₃ graded ITO anodes for acidic buffer layer free organic photovoltaics. Appl. Surf. Sci. **364**, 340–348 (2016)
2. K.P. Sibin, N. Selvakumar, A. Kumar, Design and development of ITO/Ag/ITO spectral beam splitter coating for photovoltaic-thermoelectric hybrid systems. Sol. Energy **141**, 118–126 (2017)
3. B. Murali, S. Babu, Vadivel, High performance humidity sensing properties of indium tin oxide (ITO) thin films by sol–gel spin coating method. J. Mater. Sci.: Mater. Electron. **28**, 2442–2447 (2017)
4. K. Satyendra, S. Mishra, B.D. Rani, Gupta, Surface plasmon resonance based fiber optic hydrogen sulphide gas sensor utilizing nickel oxide doped ITO thin film. Sens. Actuators B **195**, 215–222 (2014)
5. D. Zhang, I.A. Digdaya, R. Santbergen, Design and fabrication of a SiOx /ITO double-layer anti-reflective coating for heterojunction silicon solar cells. Solar Energy Mater. Solar Cells **117**, 132–138 (2013)
6. K.-H. Choi, J. Kim, Y.-J. Noh, Ag nanowire-embedded ITO films as a near-infrared transparent and flexible anode for flexible organic solar cells. Solar Energy Mater. Solar Cells **110**, 147–153 (2013)
7. M.H. Ahn, E.-S. Cho, S.J. Kwon, Effect of the duty ratio on the indium tin oxide (ITO) film deposited by in-line pulsed DC magnetron sputtering method for resistive touch panel. Appl. Surf. Sci. **258**, 1242–1248 (2011) (2011)
8. V. Craciun, D. Craciun, X. Wang, T.J. Anderson, R.K. Singh, Transparent and conducting indium tin oxide thin films grown by pulsed laser deposition at low temperatures. J.Optoelectron. Adv. Mater. **5**, 401–408 (2003)
9. S. Marikkannu, M. Kashif, N. Sethupathy, V.S. Vidhya, S. Piraman, A. Ayeshamariam, M. Bououdina, N.M. Ahmed, M. Jayachandran, Effect of substrate temperature on indium tin oxide (ITO) thin films deposited by jet nebulizer spray pyrolysis and

solar cell application. Mater. Sci. Semicond.Process. **27**, 562–568 (2014)

10. M.Moradi-Haji Jafan, M.-R. Zamani-Meymian, R. Rahimi, M. Rabbani, Effect of pyrolysis temperature on the electrical, optical, structural and morphological properties of ITO thin films prepared by a sol–gel spin coating process. Microelectron. Eng. **130**, 40–45 (2014)

11. L.L. Yang, X.D. He, F. He, Y.B. Li, S. Zhang, T. An, W.T. Zheng, Surface characterization of Ag–ITO cermet films prepared by a new sol–gel method. Thin Solid Films **517**, 4979–4983 (2009)

12. N. Xia, R.A. Gerhardt, Fabrication and characterization of highly transparent and conductive indium tin oxide films made with different solution-based methods. Mater. Res. Express **3**, 116408 (2016)

13. B.C. Yadav, K. Agrahari, S. Singh, T.P. Yadav, Fabrication and characterization of nanostructured indium tin oxide film and its application as humidity and gas sensors. J. Mater. Sci.: Mater. Electron. **27**, 4172–4179 (2016)

14. S. Yuzo Shigesato, T. Takaki, Haranou, Crystallinity and electrical properties of tin-doped indium oxide films deposited by DC magnetron sputtering. Appl. Surf. Sci. **48/49**, 269–275 (1991)

15. J.-H. Kim, J.-H. Lee, Y.-W. Heo, J.-J. Kim, Ju-O. Park, Effects of oxygen partial pressure on the preferential orientation and surface morphology of ITO films grown by RF magnetron sputtering. J. Electroceram. **23**, 169–174 (2009)

16. J. Liu, D. Wu, N. Zhang, Y. Wang, Effect of surfactants on the structure and photoelectric properties of ITO films by sol-gel method. Rare Metals **29**, 143–148 (2010)

17. J. Lee, M.A. Petruska, S. Sun, Surface modification and assembly of transparent indium tin oxide nanocrystals for enhanced conductivity. J. Phys. Chem. C **118**, 12017–120219 (2014)

18. L. Meng, M.P. dos, Santos, Properties of indium tin oxide films prepared by rf reactive magnetron sputtering at different substrate temperature. Thin Solid Films **322**, 56–62 (1998)

19. M. Parthibavarman, K. Vallalperuman, S. Sathishkumar, M. Durairaj, K. Thavamani, A novel microwave synthesis of nanocrystalline SnO_2 and its structural optical and dielectric properties. J. Mater. Sci.: Mater. Electron. **25**, 730–735 (2014)

20. J.-H. Kim, T.-Y. Seong, K.-J. Ahn, K.-B. Chung, H.-J. Seok, H.-J. Seo, H.-K. Kim, The effects of film thickness on the electrical, optical, and structural properties of cylindrical, rotating, magnetron-sputtered ITO films. Appl. Surf. Sci. **440**, 1211–1218 (2018)

21. M.T. Hammad, Effect of annealing on electrical,structural, and optical properties of sol–gel ITO thin films. Phys. Status Solidi A **206**, 2128–2132 (2009)

22. C. Wang, H. Zhang, F. Yang, Y. Fan, Q. Liu, Enhanced light scattering effect of wrinkled transparent conductive ITO thin film. RSC Adv. **7**, 25483–25487 (2017)

23. M. Premkumar, S. Vadivel, Effect of annealing temperature on structural, optical and humidity sensing properties of indium tin oxide (ITO) thin films. J. Mater. Sci.: Mater. Electron. **28**, 8460–8466 (2017)

24. Y.-H. Hyun Cho, Yun, Characterization of indium tin oxide (ITO) thin films prepared by a sol–gel spin coating process. Ceram. Int. **37**, 615–619 (2011)

25. Z. Chen, W. Li, R. Li, Y. Zhang, G. Xu, H. Cheng, Fabrication of highly transparent and conductive indium – tin oxide thin films with a high figure of merit via solution processing. Langmuir 29, 13836–13842 (2009)

26. J.H. Lee, Y.H. Kim, S.J. Ahn, T.H. Ha, H.S. Kim, Grain-size effect on the electrical properties of nanocrystalline indium tin oxide thin films. Mater. Sci. Eng., B **199**, 37–41 (2015)

27. A. Chen, K. Zhu, H. Zhong, A new investigation of oxygen flow influence on ITO thin films by magnetron sputtering. Solar Energy Mater. Solar Cells **120**, 157–162 (2014)

28. G. Haacke, New figure of merit for transparent conductors. J. Appl. Phys. **47**, 4086–4089 (1976)